HHS Public Access

Author manuscript

Toxicology. Author manuscript; available in PMC 2022 November 01.

Published in final edited form as:

Toxicology. 2021 November ; 463: 152968. doi:10.1016/j.tox.2021.152968.

Von Willebrand factor exerts hepatoprotective effects in acute but not chronic cholestatic liver injury in mice

Lauren G. Poole[1,2], **Anna-Katherine Fournier**[1], **Holly M. Cline-Fedewa**[1], **Anna K. Kopec**[1,2], **James P. Luyendyk**[1,2,3], **Dafna J. Groeneveld**[1]

[1]Department of Pathobiology & Diagnostic Investigation, Michigan State University, East Lansing, MI, USA.

[2]Institute for Integrative Toxicology, Michigan State University, East Lansing, MI, USA.

[3]Department of Pharmacology & Toxicology, Michigan State University, East Lansing, MI, USA.

Abstract

Acute and chronic liver disease are associated with substantial alterations in the hemostatic system, including elevated levels of the platelet-adhesive protein von Willebrand factor (VWF). Carbon tetrachloride-induced liver fibrosis is reduced in VWF-deficient mice, but it is unclear if VWF plays a pathologic role in all settings of liver fibrosis. Indeed, several studies suggest an anti-fibrotic role for components of the hemostatic system, including platelets, in experimental settings of bile duct fibrosis. However, the role of VWF in this specific pathology has not been examined. We tested the hypothesis that VWF exerts hepatoprotective effects in experimental bile duct injury. Wild-type and VWF-deficient ($VWF^{-/-}$) mice were challenged with the bile duct toxicant alpha-naphthylisothiocyanate (ANIT) and the impact of VWF deficiency on acute cholestatic liver injury and chronic liver fibrosis was determined. Acute ANIT (60 mg/kg, po)-induced cholestatic liver injury was associated with increased VWF plasma antigen and activity levels. VWF deficiency enhanced ANIT-induced hepatocellular injury, evidenced by increased plasma ALT activity and area of hepatocellular necrosis. Surprisingly, platelet accumulation within necrotic areas was increased in ANIT-challenged $VWF^{-/-}$ mice compared to wild-type mice. Compared to acute ANIT challenge, hepatic platelet accumulation was modest and appeared to be VWF-dependent in mice exposed to ANIT diet (0.05%) for 6 weeks. However, contrasting the role of VWF after acute ANIT challenge, VWF deficiency did not impact biliary fibrosis induced by

Corresponding Author: Dafna J. Groeneveld, PhD, Pathobiology & Diagnostic Investigation, Michigan State University, 254 Food Safety & Toxicology Building, 1129 Farm Lane, East Lansing, MI 48824, T +1 517-884-3484, groene12@cvm.msu.edu.

Authorship

Designed and conducted experiments: L.G. Poole, A.K. Fournier, H.M. Cline-Fedewa, A.K. Kopec, J.P. Luyendyk, D.J. Groeneveld

Analyzed data: L.G. Poole, A.K. Fournier, J.P. Luyendyk, D.J. Groeneveld

Interpreted the data: L.G. Poole, J.P. Luyendyk, D.J. Groeneveld

Drafted initial version of the manuscript: D.J. Groeneveld

Approved final version of the manuscript: L.G. Poole, A.K. Fournier, H.M. Cline-Fedewa, A.K. Kopec, J.P. Luyendyk, D.J. Groeneveld

Conflict of Interest

The authors have no conflicts of interest to disclose.

chronic ANIT exposure. The results suggest that VWF plays dichotomous roles in experimental acute and chronic ANIT-induced cholestatic liver injury.

Keywords

von Willebrand factor; platelets; cholestasis; ANIT; fibrosis

1. Introduction

Experimental and clinical evidence suggests that the hemostatic system contributes to liver disease progression. (Abe et al. 2007; Joshi et al. 2017a; Kopec et al. 2014; Villa et al. 2012) However, in some experimental models of liver fibrosis associated with bile duct injury and cholestasis, the hemostatic system appears to exert hepatoprotective effects. (Joshi et al. 2015; Kodama et al. 2010; Luyendyk et al. 2011a) Cholangiopathies, such as primary biliary cholangitis (PBC), are liver diseases characterized by disrupted bile flow due to damage or occlusion of bile ducts. Bile duct epithelial cell injury and/or disruption of bile flow leads to hepatocellular injury, bile duct hyperplasia and fibrosis. Exposure of rodents to the xenobiotic α-naphthylisothiocyanate (ANIT) uniquely models this type of liver pathology. (Plaa and Priestly 1976) ANIT exposure produces distinct lesions depending on the method of administration. Specifically, administration of a single dose of ANIT by oral gavage produces acute focal hepatocellular necrosis reminiscent of lesions evident after ligation of the common bile duct, often termed ‘bile infarcts. (McLean and Rees 1958) Longer term exposure (i.e., weeks) to ANIT through the diet induces mixed periportal inflammation, bile duct hyperplasia and peribiliary fibrosis. (Popper et al. 1962) To this end, ANIT exposure is a useful model to define mechanisms of liver injury initiated by intrahepatic bile duct injury.

Differences in the pathogenesis of acute and chronic ANIT-induced cholestatic liver injury have revealed context-dependent contributions of various hemostatic factors to liver pathology. For example, several experimental studies have shown that components of primary hemostasis can exert hepatoprotective effects in the setting of ANIT-induced biliary fibrosis. Complete fibrinogen deficiency increased biliary fibrosis in ANIT-challenged mice. (Luyendyk et al. 2011a) Mice expressing a mutant fibrinogen that cannot support platelet aggregation developed increased liver injury and biliary fibrosis when challenged with ANIT. (Joshi et al. 2015) Furthermore, genetic (PAR-4$^{-/-}$ mice) or pharmacologic inhibition (i.e., clopidogrel) of platelet activation increased biliary fibrosis in ANIT-challenged mice. (Joshi et al. 2015; Joshi et al. 2016) Likewise, thrombocytopenia increased hepatic fibrosis after bile duct ligation. (Kodama et al. 2010) Interestingly, other studies suggest that platelets promote hepatocellular injury in the context of acute cholestatic liver injury induced by oral ANIT challenge or bile duct ligation. (Luyendyk et al. 2011b; Sullivan et al. 2010), These studies emphasize how the precise role of components of the hemostatic system in liver injury and fibrosis depends on the details of the experimental challenge.

Platelets from patients with cholestatic liver disease were reported to be hyperactive compared with non-cholestatic liver disease patients, and expression of GP1bα, the receptor for the platelet-adhesive protein von Willebrand Factor (VWF), was increased on platelets

from patients with cholestatic liver disease. (Pihusch et al. 2002) VWF plasma levels are highly elevated in patients with various types of liver disease and often associated with disease severity.(Groeneveld et al. 2021) Prior studies have observed a role for VWF in repair of the acetaminophen-injured liver and in fibrosis induced by carbon tetrachloride. (Groeneveld et al. 2020; Joshi et al. 2017a) However, despite clinical studies suggesting potential differences in VWF and platelet activity in patients with cholestatic liver disease, the role of VWF in models of bile duct injury and cholestasis is unclear. Thus, using established experimental settings of acute and chronic ANIT exposure, we determined the effect of VWF deficiency on acute cholestatic liver injury and biliary fibrosis in mice.

2. Materials and Methods

2.1 Mice

Female $VWF^{-/-}$ mice (Denis et al. 1998) on a congenic C57Bl/6J background were originally obtained from The Jackson Laboratory (Bar Harbor, ME) and maintained by homozygous breeding. These mice have been described previously. (Denis et al. 1998) Aged-matched female wild-type mice on an identical C57Bl/6J background were used as control mice. Female mice were used for these studies because of the observation of female predominance in patients developing autoimmune liver disease where bile ducts are the primary target (e.g., PBC).(Gazda et al. 2021) Mice were between 9–13 weeks old (acute studies) or 14–20 weeks old (chronic studies). Mice were housed under a 12-h light/dark cycle, fed standard diet (Teklad 8940, Envigo), and provided drinking water *ad libitum* prior to ANIT challenge. The Institutional Animal Care and Use Committee of Michigan State University, East Lansing, USA approved all animal procedures.

2.2 Acute ANIT-induced cholestatic liver injury

Mice were fasted overnight (i.e., approximately 15 hours), before administration of 60 mg/kg ANIT (dissolved in corn oil, 6 mg/ml) or vehicle (corn oil) via oral gavage (10 ml/kg), as described previously. (Sullivan et al. 2010) Acute ANIT challenge studies were performed in two independent cohorts of mice of each genotype (n = 5–7 for vehicle treated mice, n = 13–14 for ANIT-challenged mice). Blood and liver samples were collected 48 hours after ANIT administration. Blood was collected under isoflurane anesthesia by exsanguination from the caudal vena cava into a syringe containing sodium citrate (0.38% final) for the collection of plasma. To collect serum, additional blood was collected into a syringe without anticoagulant. Samples were centrifuged at 4000 × *g* for 10 minutes (for plasma) or at 10,000 × *g* for 2 minutes (for serum) and were subsequently stored at −80°C. Livers were rinsed in PBS and the left lateral lobe was fixed in 10% neutral-buffered formalin for prior to routine processing. The remaining liver was snap frozen in liquid nitrogen.

2.3 Chronic ANIT-induced cholestatic liver disease

Custom diets were prepared by Dyets, Inc. (Bethlehem, PA). Standard rodent chow diet (Teklad 8940) was formulated to contain 0.05% ANIT (Sigma-Aldrich, St. Louis, MO). Mice were fed either control diet (Teklad 8940) (n = 4–6 mice) or chow containing ANIT

(ANIT diet, 0.05% ANIT) (n = 10 mice) for 6 weeks as previously described (Joshi et al. 2017b), at which time blood and livers were collected as described above.

2.4 Measurement of hepatocellular injury, necrosis, and fibrosis

Formalin-fixed, paraffin-embedded livers were sectioned at 5 μm and stained with hematoxylin and eosin (H&E),picrosirius red (PSR), cytokeratin-19 (CK-19) antigen, or cleaved caspase 3 as described previously (Joshi et al. 2015; Kopec et al. 2018) by the MSU Investigative Histopathology Laboratory, a division of Human Pathology. Neutrophil infiltration after acute ANIT challenge was assessed by IHC staining of sectioned livers using *InVivo*Mab anti-mouse Ly6G antibody (1 μg/ml final dilution, Clone 1A8, BioXcell, West Lebanon, NH) and PromARK Micro-polymer Detection System (Biocare medical, CA). For quantification of focal hepatocellular necrosis (i.e. bile infarcts), PSR staining (collagen deposits), or CK-19 (biliary hyperplasia) images of stained liver sections were captured using a Virtual Slide System VS110 (Olympus, Hicksville, NY) with a 20X objective. One section of the entire left lateral lobe was evaluated. The area occupied by focal hepatocellular necrosis was determined by manual outlining using Olympus cellSens Dimension software (version 1.15, Olympus Corporation). The area of liver necrosis was measured and compared with the total area of the left lateral lobe. Percentage of necrosis, total number of necrotic lesions, and the average lesion size were determined. For the quantification of collagen deposition (PSR) and CK-19 staining, the percentage area of positive PSR or CK-19 staining was determined in an automated and unbiased fashion using a batch macro and the color de-convolution tool in Fiji (ImageJ, National Institutes of Health). (Schindelin et al. 2012) Serum alanine aminotransferase (ALT) and alkaline phosphatase (ALP) activities and serum direct bilirubin levels were determined using commercial reagents (ThermoFisher, Waltham, MA; Pointe Scientific, Canton, MI).

2.5 Immunofluorescent labeling of liver sections

VWF and platelets were detected by immunofluorescent labeling of frozen liver sections, as described previously. (Groeneveld et al. 2020) Slides were scanned using a Virtual Slide System VS110 (Olympus) with a 20× objective. The area of positive VWF and platelet labeling was quantified using a batch macro and color de-convolution tool in Fiji (ImageJ) as previously described. (Groeneveld et al. 2020) For quantification of platelet accumulation within necrotic lesions after acute ANIT challenge, the area occupied by focal hepatocellular necrosis in each image was manually quantified by rough outline of areas in which the loss of hepatocellular DAPI was evident using the selection tool in Fiji (ImageJ). Platelet staining within each area was determined and CD41 staining per necrotic lesion calculated using the threshold and particle analyzing tool in Fiji (ImageJ).

2.6 Measurement of VWF plasma levels and activity

Plasma VWF antigen levels were determined by ELISA, as previously described. (Groeneveld et al. 2020) Pooled normal mouse plasma was utilized to develop a standard curve. VWF binding to immobilized collagen (VWF:Collagen Binding) was assessed using a VWF:CB assay (VWF:CBA), as described with slight modifications. (Lisman et al. 2006) In brief, collagen type III (Type X, C4407, Sigma) was dissolved in 0.05M acetic acid to 1 mg/ml. Plates were coated with collagen overnight (diluted to 10μg/ml in 50mM carbonate

buffer, pH 9.6, 115 μl/well), and after washing the plate was blocked for 1h at 37 °C with blocking buffer (3% bovine serum albumin, 0.1% Tween20, in PBS). The standard curve was generated by serial dilution of normal pooled mouse plasma (1:5 to 1:320 in blocking buffer). Plasma samples (100 μl/well) were incubated for 2h at 37 °C, and after washing the plate, bound VWF was detected using a peroxidase-conjugated anti-human VWF antibody (DAKO, P0226) (1:1000 in blocking buffer, 100 μl/well, 1.5h incubation at 37 °C). Peroxidase activity was assessed using TMB substrate set (421101, Biolegend) according to the manufacturer's instruction.

2.7 RNA isolation, cDNA synthesis and quantitative real-time PCR (qPCR)

Small sections (~20 mg) of the liver lobes were collected for RNA isolation and snap frozen in liquid nitrogen. RNA isolation, cDNA synthesis and qPCR were performed as described. (Kopec et al. 2017) Detection and quantification of select mRNAs by SYBR Green qPCR were performed using primers described previously. (Poole et al. 2018) The expression of each gene was normalized to the geometric mean Ct of three housekeeping genes, i.e., *Ubc*, *Hprt* and *Gapdh,* and relative fold change was determined with the ΔΔCt method, as described previously.(Vandesompele et al. 2002) All fold changes were normalized relative to expression in wild-type mice. A complete list of all gene names and primer sequences is provided in Supplementary Table 1.

2.8 Statistics

Statistical analyses were performed with GraphPad Prism v.8 (San Diego, CA) software package. Continuous variables are presented as mean and individual data is plotted. Comparison of two groups was performed using Student's *t* test. Comparison of three or more groups was performed using two-way analysis of variance (ANOVA) with Bonferroni *post-hoc* test. In cases where data were not normally distributed, data were log-transformed to achieve a normal distribution before testing. Spearman's correlation was used to determine the strength of association between VWF parameters and liver injury markers. Significance was set at $P < 0.05$.

3. Results

3.1 VWF levels are increased in mice with ANIT-induced acute cholestatic injury.

Compared with vehicle-challenged mice, plasma VWF antigen (VWF:Ag) levels were increased 48 hours after ANIT challenge (Table 1). In line with the increase in VWF antigen level, VWF collagen binding (VWF:CB), an index of VWF activity, increased after ANIT challenge in wild-type mice (Table 1). The ratio of VWF:CB activity to VWF:Ag was similar between ANIT-challenged mice and vehicle-challenged mice (Table 1), indicating that the increase in VWF activity was likely a reflection of increased plasma VWF antigen. A strong positive correlation between VWF:Ag levels and severity of cholestatic liver injury was observed, as assessed by serum ALT ($r = 0.83$, $p < 0.001$) and ALP activities ($r = 0.84$, $p < 0.001$) (Fig 1A, B). Similarly, a strong positive correlation was observed between VWF activity and serum ALT activity ($r=0.85$, $p <0.001$) and ALP activity ($r=0.87$, $p<0.001$) (Fig 1C, D). Immunofluorescent labeling revealed VWF localized around the large vessel walls in liver sections from vehicle- and ANIT-challenged mice (white arrows, Fig 1E),

likely reflecting its expression by vascular endothelial cells Robust VWF accumulation was also evident at the periphery of areas of hepatocellular necrosis 48 hours after ANIT challenge (white triangles, Fig 1E). Taken together, the results indicate that ANIT-induced liver damage is associated with increased plasma VWF concentration and hepatic VWF deposition.

3.2 VWF deficiency exacerbates acute ANIT-induced cholestatic liver injury.

Next, we used a genetic approach to determine the role of VWF in ANIT-induced acute cholestatic liver injury. Serum ALT activity was significantly increased in ANIT-challenged VWF$^{-/-}$ mice compared to ANIT-challenged wild-type mice (Fig 2A). Serum ALP activity was increased in both genotypes of mice after ANIT challenge, but there was no significant difference between ANIT-challenged wild-type mice and ANIT-challenged VWF$^{-/-}$ mice (Fig 2B). Serum bilirubin concentration only increased significantly in ANIT-challenged VWF$^{-/-}$ mice compared to vehicle-treated VWF$^{-/-}$ mice and was not significantly different after ANIT challenge in wild-type and VWF$^{-/-}$ mice (Fig 2C). Hepatocellular necrosis induced by a single dose of ANIT is characterized by multifocal necrotic lesions (i.e. “bile infarcts”). (Luyendyk et al. 2009) Consistent with increased serum ALT activity, the area of hepatic necrosis was significantly greater in ANIT-challenged VWF$^{-/-}$ mice compared with ANIT-challenged wild-type mice (Fig 2D). This was a consequence of a significant increase in lesion frequency (Fig 2E,H) and a trend towards increase in lesion size (Fig 2G,H) in ANIT-challenged VWF$^{-/-}$ mice. Moreover, red blood cell infiltration in bile infarcts was clearly increased in ANIT-challenged VWF$^{-/-}$ mice (indicated by black triangles, Fig 2H). Abundant neutrophil infiltration was observed within areas of hepatocellular necrosis in ANIT-challenged wild-type mice. Interestingly, the pattern of neutrophil accumulation in ANIT-challenged VWF−/− mice included an apparent increase in neutrophil accumulation in neighboring non-necrotic parenchymal tissue (suppl Fig 1A). Notably, marked biliary hyperplasia was evident after ANIT challenge. However, there was no obvious difference in CK-19 staining in livers of wild-type and VWF$^{-/-}$ mice after ANIT challenge (suppl Fig 1B). Consistent with prior studies evaluating the role of apoptosis in models of acute cholestatic liver damage, apoptotic cells (cleaved caspase 3) were sporadic and irrespective of genotype or ANIT challenge (Supplemental Fig. 2), suggesting apoptosis was not a predominant form of cell death. Platelet accumulation in livers of ANIT-challenged wild-type mice was predominantly within areas of hepatocellular necrosis and there was some platelet-VWF colocalization (white arrows, Fig 3A). Because VWF serves as an adhesion protein for platelets, we anticipated a reduction in platelet accumulation in areas of necrosis in ANIT-challenged VWF$^{-/-}$ mice. To our surprise, VWF deficiency increased platelet accumulation within necrotic lesions, indicating VWF is not essential for hepatic platelet accumulation after acute ANIT challenge (Fig 3A, B).

3.3 Impact of chronic ANIT exposure on plasma and hepatic VWF.

Exposure of mice to ANIT via diet (0.05%) induces bile duct hyperplasia and peribiliary fibrosis. (Plaa and Priestly 1976) A slight but statistically significant increase in plasma VWF antigen levels was evident in wild-type mice fed ANIT diet (6 weeks) (Fig 4A). Likewise, plasma VWF activity increased after chronic ANIT exposure (Fig 4B). Like the changes observed in acute ANIT challenge, chronic ANIT exposure showed a normal

VWF:CB to VWF:Ag ratio (Fig 4C), suggesting that changes in VWF activity are likely a consequence of increased plasma VWF antigen levels, and not because of altered proteolysis by ADAMTS-13. VWF labeling, distributed in a granular pattern, marked the intimal lining of large vessels (i.e. portal and central veins) in mice fed control diet (white arrow, Fig 4E), reflecting its known expression by vascular endothelial cells Hepatic VWF deposits increased significantly in mice fed ANIT diet (Fig 4D), with apparent increase in intensity along the endothelial lining of blood vessels and within the areas that resembled biliary hyperplasia (white triangles, Fig 4E). Moreover, an increase in small spots reflecting VWF deposits were observed in the liver parenchyma (Fig 4E), suggesting a potential increase in hepatic platelet accumulation.

3.4 VWF contributes to hepatic platelet accumulation driven by chronic ANIT exposure.

Chronic exposure of mice to ANIT through diet is associated with increased coagulation activation and hepatic platelet accumulation is evident in livers of ANIT-challenged mice. (Joshi et al. 2015) Scattered platelet staining was mostly confined to larger vessels in both wild-type and $VWF^{-/-}$ mice fed control diet. An increase in hepatic platelet accumulation, albeit modest, was evident in livers of wild-type mice fed ANIT diet (Fig 5A–C). Interestingly, hepatic platelet accumulation was significantly reduced in $VWF^{-/-}$ mice that were fed ANIT diet compared with wild-type mice fed ANIT diet (Fig 5A–C). Thus, in contrast to acute ANIT challenge, VWF contributes to hepatic platelet accumulation in mice exposed to ANIT via the diet.

3.5 VWF deficiency reduces chronic ANIT-induced liver injury but not fibrosis in mice.

Prior studies suggest the components of the hemostatic system, including platelets, exert hepatoprotective effects in mice exposed chronically to ANIT. (Joshi et al. 2016) Compared to acute ANIT challenge, elevation in liver enzymes in serum is minimal. However, to our surprise, serum ALT and ALP activity were reduced in $VWF^{-/-}$ mice fed ANIT diet vs. wild-type mice fed ANIT diet (Fig 6A, B). VWF deficiency did not affect hepatic expression of the profibrogenic genes *Col1a1* and *Itgb6* in mice fed ANIT diet (Fig 6C, D), nor was hepatic collagen deposition, indicated by picrosirius red staining and quantification, affected by VWF deficiency in mice fed ANIT diet (Fig 6E, F). The results suggest that VWF deficiency does not affect liver fibrosis induced by chronic ANIT exposure.

4. Discussion

Several studies have suggested that platelets play diverse roles in liver damage caused by intrahepatic bile duct injury. In the case of acute ANIT-induced cholestatic liver injury in rodents, studies suggest platelets exacerbate hepatocellular necrosis (Sullivan et al. 2010), although this may depend on the timing of platelet inhibition/depletion and time point examined. Notably, the precise mechanism driving platelet accumulation in the injured liver is unknown. Prior studies examining the impact of PAR or fibrinogen deficiency in ANIT-challenged mice did not examine hepatic platelet accumulation (Luyendyk et al. 2011b). To our surprise, and the opposite of our hypothesis, VWF deficiency enhanced platelet accumulation within necrotic lesions, even when we corrected for the increased lesion size

in ANIT-challenged VWF$^{-/-}$ mice. This result clearly indicates that the mechanisms driving platelet accumulation in injured liver after acute ANIT challenge do not require VWF.

In line with our previous studies showing damaging effects of platelets in acute ANIT-induced liver injury (Sullivan et al. 2010), our results suggest the surprising possibility that VWF deficiency paradoxically enhances platelet accumulation and hepatic necrosis in this model. Other proteins such as fibrinogen, also deposited in areas of necrosis in livers of ANIT-challenged mice, may promote additional hepatic platelet accumulation in the absence of VWF. Alternatively, VWF deficiency may drive ANIT-induced acute liver injury via mechanisms independent of platelets. Indeed, an increase in hepatic platelet accumulation occurring because of necrosis itself cannot be excluded. Although VWF is best known for its role in hemostasis, several other novel biological functions for VWF have been identified in recent years. Recently, it was shown that VWF plays an important role in regulating wound healing. (Ishihara et al. 2019) Using a dermal skin wound model, VWF was shown to stimulate wound healing by promoting local angiogenesis and tissue regeneration. (Ishihara et al. 2019) Interestingly, while these results seem to contrast previous studies in which it was shown that VWF inhibits angiogenesis (Starke et al. 2011), *in vivo* data from other animal models suggest a dichotomous role of VWF in regulating angiogenesis depending on the experimental setting. (de Vries et al. 2017; Hillgruber et al. 2014; Xu et al. 2017) It is plausible that VWF could inhibit acute ANIT-induced liver injury by promoting local angiogenesis or repair/regeneration.

Previous studies have suggested that chronic ANIT exposure is associated with hepatic platelet accumulation. (Joshi et al. 2015) Compared to the marked platelet accumulation we observed in areas of hepatocellular necrosis after acute ANIT challenge, long exposure to ANIT produced a much more modest and apparently panlobular platelet accumulation. Interestingly, VWF deficiency significantly reduced hepatic platelet accumulation in mice fed ANIT diet. Prior studies using various genetic and pharmacologic strategies to inhibit platelet activation/aggregation have suggested potential protective effects of platelets in the ANIT diet model, although it is worth noting that hepatic platelet accumulation was not evaluated in those studies. (Joshi et al. 2015; Joshi et al. 2016) Notably, the reduction in hepatic platelet accumulation in VWF$^{-/-}$ mice fed ANIT diet did not have a significant effect on biliary fibrosis. It could be that the protective function of platelets in this context is less related to their hepatic accumulation, and more to their release of specific granule contents. Indeed, in contrast to models of acute hepatotoxicity, which are associated with abundant hepatic platelet aggregates (Groeneveld et al. 2020), the pattern of platelet accumulation in livers of mice fed ANIT diet was clearly different, with only a slight increase in what appeared to be individual platelets or small aggregates. An alternative explanation for this different accumulation pattern, seemingly disconnected from the primary site of pathology (i.e., portal tracts), is an increase in clearance of platelets from the circulation induced by ANIT exposure. Binding of VWF to platelets is one of the major mechanisms of platelet clearance (Quach et al. 2018), and this could explain why VWF deficiency was associated with reduced hepatic platelet accumulation.

The modest increases in liver enzymes in serum was reduced in VWF$^{-/-}$ mice fed ANIT diet, yet there was no effect of VWF deficiency on development of liver fibrosis in mice

challenged with ANIT diet. This further supports the concept that hepatocellular injury and biliary fibrosis are mechanistically distinct lesions, revealed by differential connections of each lesion to dose in this model. (Joshi et al. 2017b) Likewise, administration of the platelet inhibitor clopidogrel exacerbated biliary fibrosis, but had no effect on hepatocellular injury after chronic ANIT challenge.(Joshi et al. 2016) The observation that these two liver pathologies are disconnected is important for interpretation of studies investigating the role of hemostasis in liver fibrosis. Specifically, we may not expect a reduction in serum liver enzymes in $VWF^{-/-}$ mice fed ANIT diet to foreshadow a reduction in liver fibrosis. In contrast, in other modes where persistent hepatocellular injury is connected to fibrosis, the outcome may be different. Indeed, we have showed previously that VWF deficiency reduced liver fibrosis induced by chronic administration of the hepatotoxicant carbon tetrachloride (CCl_4) (Joshi et al. 2017a). These results suggest that the role of VWF in hepatic injury and fibrosis is specific to the toxicant administered and our studies underline the need to consider the different etiologies and precise chemical challenge when comparing the role of specific hemostatic proteins or interventions in different models of chronic liver injury.

Clinical studies have shown that patients with acute or chronic liver disease have substantial alterations in their hemostatic system, including highly elevated levels of VWF in plasma. (Bos et al. 2019; Hugenholtz et al. 2013; Lisman and Porte 2010; Lisman and Stravitz 2015; Takaya et al. 2017) However, the ratio of VWF activity to antigen is reduced in patients (Hugenholtz et al. 2013), indicating that VWF activity does not increase to the same extent as protein levels. In some experimental settings, such as acute acetaminophen overdose (Groeneveld et al. 2020), the VWF:CB/VWF:Ag ratio is also reduced. Interestingly, this was not the case for acute ANIT challenge or ANIT diet exposure, where plasma VWF levels increased without a change in VWF:CB/VWF:Ag ratio. Clinical studies have shown that patients with liver disease have reduced plasma levels of the ADAMTS-13, an enzyme that reduces VWF activity. We cannot exclude a change in ADAMTS13 contributing to deposition of high molecular weight multimer VWF in the injured liver. However, the results suggest that VWF antigen, not changes in VWF activity, is a primary driver of increased plasma VWF activity after ANIT challenge. Most clinical studies assessing hemostatic changes are performed using patient cohorts with mixed etiologies, the precise effect of cholestatic liver disease on changes in VWF parameters is not well defined. Bos et al. (Bos et al. 2019) recently showed that VWF antigen levels were similarly increased across all etiologies, although VWF:CB/VWF:Ag ratio was not assessed. Interestingly, VWF staining of the endothelial lining of large vessels was clearly more intense in liver sections from mice fed ANIT diet. This could indicate that chronic ANIT exposure leads to an increase in VWF expression or endothelial cell activation. How this relates to the perceived hypercoagulable state in patients with cholestatic liver disorders (Pihusch et al. 2002) and the connection to VWF activity remains to be determined.

Our studies show that both acute ANIT challenge and chronic exposure to ANIT diet are associated with increased plasma and hepatic VWF levels and differential patterns of platelet accumulation in the injured liver. VWF deficiency exacerbated acute ANIT cholestatic liver injury whereas there was no significant effect of VWF deficiency on biliary fibrosis induced by ANIT diet. Our studies did not identify the mechanistic basis for these differences. Isolating the mechanisms whereby VWF participates in ANIT hepatotoxicity may be best

uncovered by additional studies with emerging tools capable of targeting specific VWF functional domains or its targets. In addition, it seems plausible that key insight from these studies could lead to generation of *in vitro* settings in which *in vivo* mediators of hepatotoxicity are paired with cellular and soluble mediators of hemostasis. The integration of these approaches is likely to facilitate discovery of the mechanisms for the context-dependent contribution of VWF, and other hemostatic proteins, in the pathogenesis of acute and chronic liver injury.

Supplementary Material

Refer to Web version on PubMed Central for supplementary material.

Financial Support

This work was supported by an EHA Research Grant from the European Hematology Association (EHA) to DG, a grant from the National Institutes of Health (NIH) to JPL (R01 ES017537), and F32 DK121423 to LP, and support from the USDA National Institute of Food and Agriculture. The content is solely the responsibility of the authors and does not necessarily represent the official views of the NIEHS, NIDDK or the NIH.

References

Abe W, Ikejima K, Lang T, Okumura K, Enomoto N, Kitamura T, Takei Y and Sato N 2007. Low molecular weight heparin prevents hepatic fibrogenesis caused by carbon tetrachloride in the rat. J Hepatol 46, 286–294. [PubMed: 17166617]

Bos S, van den Boom B, Kamphuisen PW, Adelmeijer J, Blokzijl H, Schreuder T and Lisman T 2019. Haemostatic Profiles are Similar across All Aetiologies of Cirrhosis. Thromb Haemost 119, 246–253. [PubMed: 30609442]

de Vries MR, Peters EAB, Quax PHA and Nossent AY 2017. von Willebrand factor deficiency leads to impaired blood flow recovery after ischaemia in mice. Thromb Haemost 117, 1412–1419. [PubMed: 28382367]

Denis C, Methia N, Frenette PS, Rayburn H, Ullman-Cullere M, Hynes RO and Wagner DD 1998. A mouse model of severe von Willebrand disease: defects in hemostasis and thrombosis. Proc Natl Acad Sci U S A 95, 9524–9529. [PubMed: 9689113]

Gazda J, Drazilova S, Janicko M and Jarcuska P 2021. The Epidemiology of Primary Biliary Cholangitis in European Countries: A Systematic Review and Meta-Analysis. Can J Gastroenterol Hepatol 2021, 9151525. [PubMed: 34239845]

Groeneveld D, Cline-Fedewa H, Baker KS, Williams KJ, Roth RA, Mittermeier K, Lisman T, Palumbo JS and Luyendyk JP 2020. Von Willebrand factor delays liver repair after acetaminophen-induced acute liver injury in mice. J Hepatol 72, 146–155. [PubMed: 31606553]

Groeneveld D, Poole LG and Luyendyk JP 2021. Targeting von Willebrand factor in liver diseases: a novel therapeutic strategy? J Thromb Haemost.

Hillgruber C, Steingräber AK, Pöppelmann B, Denis CV, Ware J, Vestweber D, Nieswandt B, Schneider SW and Goerge T 2014. Blocking von Willebrand factor for treatment of cutaneous inflammation. J Invest Dermatol 134, 77–86. [PubMed: 23812299]

Hugenholtz GC, Adelmeijer J, Meijers JC, Porte RJ, Stravitz RT and Lisman T 2013. An unbalance between von Willebrand factor and ADAMTS13 in acute liver failure: implications for hemostasis and clinical outcome. Hepatology 58, 752–761. [PubMed: 23468040]

Ishihara J, Ishihara A, Starke RD, Peghaire CR, Smith KE, McKinnon TAJ, Tabata Y, Sasaki K, White MJV, Fukunaga K, Laffan MA, Lutolf MP, Randi AM and Hubbell JA 2019. The heparin binding domain of von Willebrand factor binds to growth factors and promotes angiogenesis in wound healing. Blood 133, 2559–2569. [PubMed: 30975637]

Joshi N, Kopec AK, O'Brien KM, Towery KL, Cline-Fedewa H, Williams KJ, Copple BL, Flick MJ and Luyendyk JP 2015. Coagulation-driven platelet activation reduces cholestatic liver injury and fibrosis in mice. J Thromb Haemost 13, 57–71. [PubMed: 25353084]

Joshi N, Kopec AK, Ray JL, Cline-Fedewa H, Groeneveld DJ, Lisman T and Luyendyk JP 2017a. Von Willebrand factor deficiency reduces liver fibrosis in mice. Toxicol Appl Pharmacol 328, 54–59. [PubMed: 28527913]

Joshi N, Kopec AK, Ray JL and Luyendyk JP 2016. Inhibition of PAR-4 and P2Y12 receptor-mediated platelet activation produces distinct hepatic pathologies in experimental xenobiotic-induced cholestatic liver disease. Toxicology 365, 9–16. [PubMed: 27475285]

Joshi N, Ray JL, Kopec AK and Luyendyk JP 2017b. Dose-dependent effects of alpha-naphthylisothiocyanate disconnect biliary fibrosis from hepatocellular necrosis. J Biochem Mol Toxicol 31, 1–7.

Kodama T, Takehara T, Hikita H, Shimizu S, Li W, Miyagi T, Hosui A, Tatsumi T, Ishida H, Tadokoro S, Ido A, Tsubouchi H and Hayashi N 2010. Thrombocytopenia exacerbates cholestasis-induced liver fibrosis in mice. Gastroenterology 138, 2487–2498, 2498.e2481–2487. [PubMed: 20206174]

Kopec AK, Joshi N, Cline-Fedewa H, Wojcicki AV, Ray JL, Sullivan BP, Froehlich JE, Johnson BF, Flick MJ and Luyendyk JP 2017. Fibrin(ogen) drives repair after acetaminophen-induced liver injury via leukocyte alphaMbeta2 integrin-dependent upregulation of Mmp12. J Hepatol 66, 787–797. [PubMed: 27965156]

Kopec AK, Joshi N, Towery KL, Kassel KM, Sullivan BP, Flick MJ and Luyendyk JP 2014. Thrombin inhibition with dabigatran protects against high-fat diet-induced fatty liver disease in mice. J Pharmacol Exp Ther 351, 288–297. [PubMed: 25138021]

Kopec AK, Spada AP, Contreras PC, Mackman N and Luyendyk JP 2018. Caspase Inhibition Reduces Hepatic Tissue Factor-Driven Coagulation In Vitro and In Vivo. Toxicol Sci 162, 396–405. [PubMed: 29228388]

Lisman T and Porte RJ 2010. Rebalanced hemostasis in patients with liver disease: evidence and clinical consequences. Blood 116, 878–885. [PubMed: 20400681]

Lisman T, Raynal N, Groeneveld D, Maddox B, Peachey AR, Huizinga EG, de Groot PG and Farndale RW 2006. A single high-affinity binding site for von Willebrand factor in collagen III, identified using synthetic triple-helical peptides. Blood 108, 3753–3756. [PubMed: 16912226]

Lisman T and Stravitz RT 2015. Rebalanced Hemostasis in Patients with Acute Liver Failure. Semin Thromb Hemost 41, 468–473. [PubMed: 26049071]

Luyendyk JP, Cantor GH, Kirchhofer D, Mackman N, Copple BL and Wang R 2009. Tissue factor-dependent coagulation contributes to alpha-naphthylisothiocyanate-induced cholestatic liver injury in mice. Am J Physiol Gastrointest Liver Physiol 296, G840–849. [PubMed: 19179621]

Luyendyk JP, Kassel KM, Allen K, Guo GL, Li G, Cantor GH and Copple BL 2011a. Fibrinogen deficiency increases liver injury and early growth response-1 (Egr-1) expression in a model of chronic xenobiotic-induced cholestasis. Am J Pathol 178, 1117–1125. [PubMed: 21356363]

Luyendyk JP, Mackman N and Sullivan BP 2011b. Role of fibrinogen and protease-activated receptors in acute xenobiotic-induced cholestatic liver injury. Toxicol Sci 119, 233–243. [PubMed: 20974703]

McLean MR and Rees KR 1958. Hyperplasia of bile-ducts induced by alpha-naphthyl-isothiocyanate: experimental biliary cirrhosis free from biliary obstruction. J Pathol Bacteriol 76, 175–188. [PubMed: 13576358]

Pihusch R, Rank A, Göhring P, Pihusch M, Hiller E and Beuers U 2002. Platelet function rather than plasmatic coagulation explains hypercoagulable state in cholestatic liver disease. J Hepatol 37, 548–555. [PubMed: 12399218]

Plaa GL and Priestly BG 1976. Intrahepatic cholestasis induced by drugs and chemicals. Pharmacol Rev 28, 207–273. [PubMed: 16281]

Poole LG, Pant A, Baker KS, Kopec AK, Cline-Fedewa HM, Iismaa SE, Flick MJ and Luyendyk JP 2018. Chronic liver injury drives non-traditional intrahepatic fibrin(ogen) crosslinking via tissue transglutaminase. J Thromb Haemost.

Popper H, Rubin E and Schaffner F 1962. The problem of primary biliary cirrhosis. Am J Med 33, 807–810. [PubMed: 13972306]

Quach ME, Chen W and Li R 2018. Mechanisms of platelet clearance and translation to improve platelet storage. Blood 131, 1512–1521. [PubMed: 29475962]

Schindelin J, Arganda-Carreras I, Frise E, Kaynig V, Longair M, Pietzsch T, Preibisch S, Rueden C, Saalfeld S, Schmid B, Tinevez JY, White DJ, Hartenstein V, Eliceiri K, Tomancak P and Cardona A 2012. Fiji: an open-source platform for biological-image analysis. Nat Methods 9, 676–682. [PubMed: 22743772]

Starke RD, Ferraro F, Paschalaki KE, Dryden NH, McKinnon TA, Sutton RE, Payne EM, Haskard DO, Hughes AD, Cutler DF, Laffan MA and Randi AM 2011. Endothelial von Willebrand factor regulates angiogenesis. Blood 117, 1071–1080. [PubMed: 21048155]

Sullivan BP, Wang R, Tawfik O and Luyendyk JP 2010. Protective and damaging effects of platelets in acute cholestatic liver injury revealed by depletion and inhibition strategies. Toxicol Sci 115, 286–294. [PubMed: 20133375]

Takaya H, Yoshiji H, Kawaratani H, Sakai K, Matsumoto M, Fujimura Y and Fukui H 2017. Decreased activity of plasma ADAMTS13 are related to enhanced cytokinemia and endotoxemia in patients with acute liver failure. Biomedical reports 7, 277–285. [PubMed: 28894574]

Vandesompele J, De Preter K, Pattyn F, Poppe B, Van Roy N, De Paepe A and Speleman F 2002. Accurate normalization of real-time quantitative RT-PCR data by geometric averaging of multiple internal control genes. Genome Biol 3, RESEARCH0034. [PubMed: 12184808]

Villa E, Cammà C, Marietta M, Luongo M, Critelli R, Colopi S, Tata C, Zecchini R, Gitto S, Petta S, Lei B, Bernabucci V, Vukotic R, De Maria N, Schepis F, Karampatou A, Caporali C, Simoni L, Del Buono M, Zambotto B, Turola E, Fornaciari G, Schianchi S, Ferrari A and Valla D 2012. Enoxaparin prevents portal vein thrombosis and liver decompensation in patients with advanced cirrhosis. Gastroenterology 143, 1253–1260.e1254. [PubMed: 22819864]

Xu H, Cao Y, Yang X, Cai P, Kang L, Zhu X, Luo H, Lu L, Wei L, Bai X, Zhu Y, Zhao BQ and Fan W 2017. ADAMTS13 controls vascular remodeling by modifying VWF reactivity during stroke recovery. Blood 130, 11–22. [PubMed: 28428179]

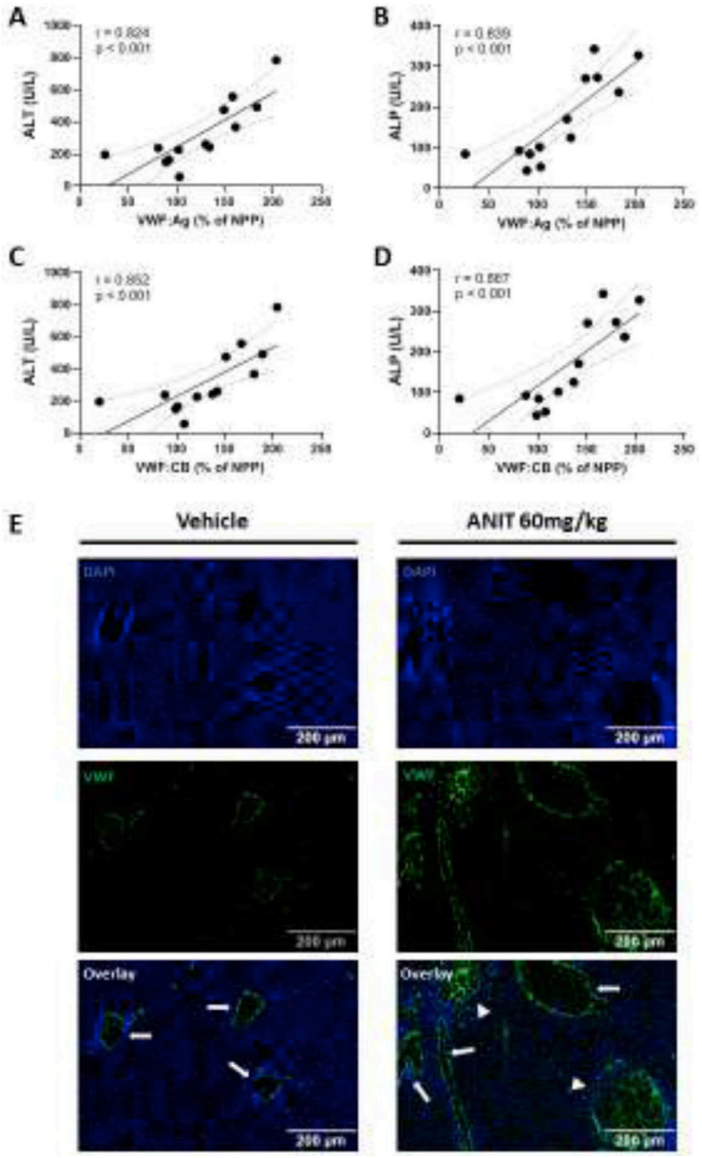

Figure 1. Impact of ANIT-induced acute liver injury on plasma and hepatic VWF.

Fasted female wild-type mice were challenged with vehicle (corn oil) or ANIT (60mg/kg, p.o.) and samples were collected 48 hours later. Blood was collected to assess serum alanine aminotransferase (ALT) and alkaline phosphatase (ALP) and VWF parameters in plasma, and livers were collected to assess hepatic VWF deposition. VWF plasma antigen (VWF:Ag) levels in wild-type mice after ANIT challenge showed a significant correlation with both serum ALT levels (A) as well as serum ALP levels (B). VWF activity (VWF:CB), assessed with a collagen binding assay, in plasma samples from wild-type ANIT-challenged mice showed a significant correlation with both ALT levels (C) and ALP levels (D). VWF:Ag and VWF:CB levels are expressed as % of normal pooled mouse plasma which was set at 100%. (E) Representative images of VWF (in green) and cell nuclei (in blue) in liver sections of mice challenged with vehicle (left panels) or ANIT (right panels). White arrows mark VWF staining of the endothelial lining, white triangles mark VWF

staining within necrotic lesions. Dashed lines indicate 95% Confidence bands for best-fit, and individual animals are plotted (n = 13 mice per group for panels A-D).

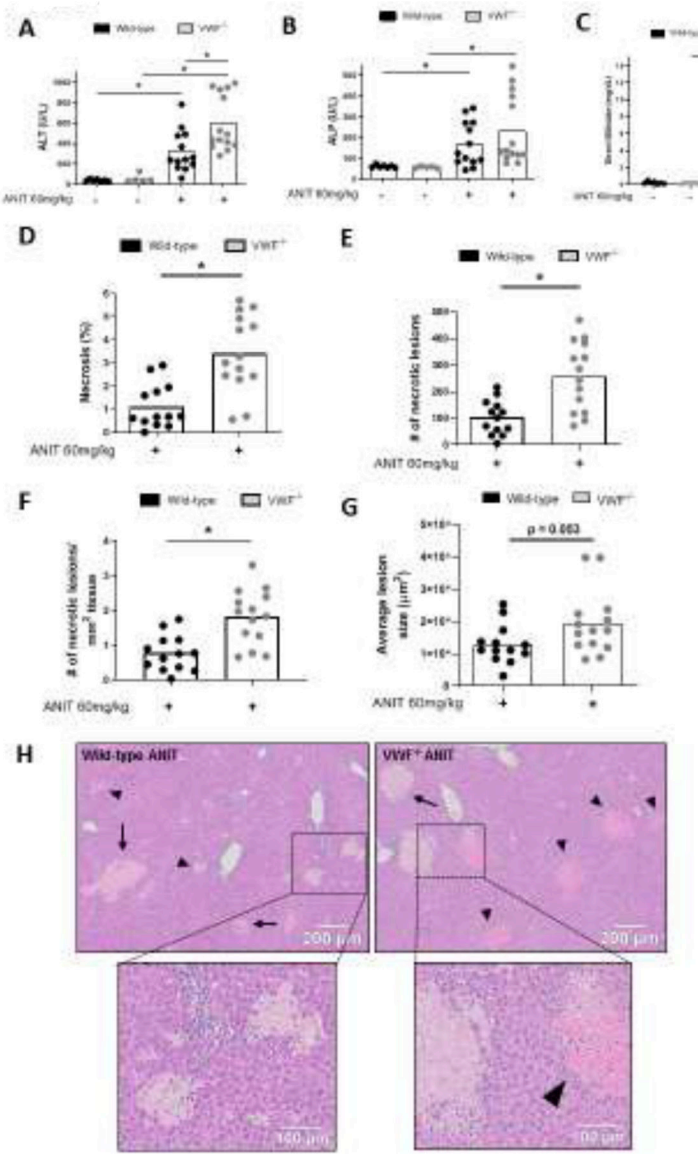

Figure 2. VWF deficiency exacerbates ANIT-induced acute liver injury in mice.

Fasted female wild-type and VWF$^{-/-}$ mice were challenged with vehicle (corn oil) or ANIT (60mg/kg, po) and 48 later blood and livers were collected to assess liver and biliary injury. (A) Serum alanine aminotransferase (ALT) activity in vehicle- and ANIT-challenged mice. (B) Serum alkaline phosphate (ALP) activity in vehicle- and ANIT-challenged mice. (C) Serum direct bilirubin levels. Quantification of (D) total hepatocellular necrosis, (E) total number of necrotic lesions in the entire left lateral lobe, (F) number of necrotic lesions per mm^2 liver tissue, and (G) average size of necrotic lesions in left lateral lobes of ANIT-exposed wild-type and VWF$^{-/-}$ mice. (H) Representative photomicrographs of H&E-stained liver sections show areas of hepatocellular necrotic lesions (pink color, black arrows). Black triangles indicate necrotic lesions with blood cell infiltration (dark pink color within necrotic lesion). Bars represent mean and individual animals are plotted (n = 13–14 mice). * p <0.05.

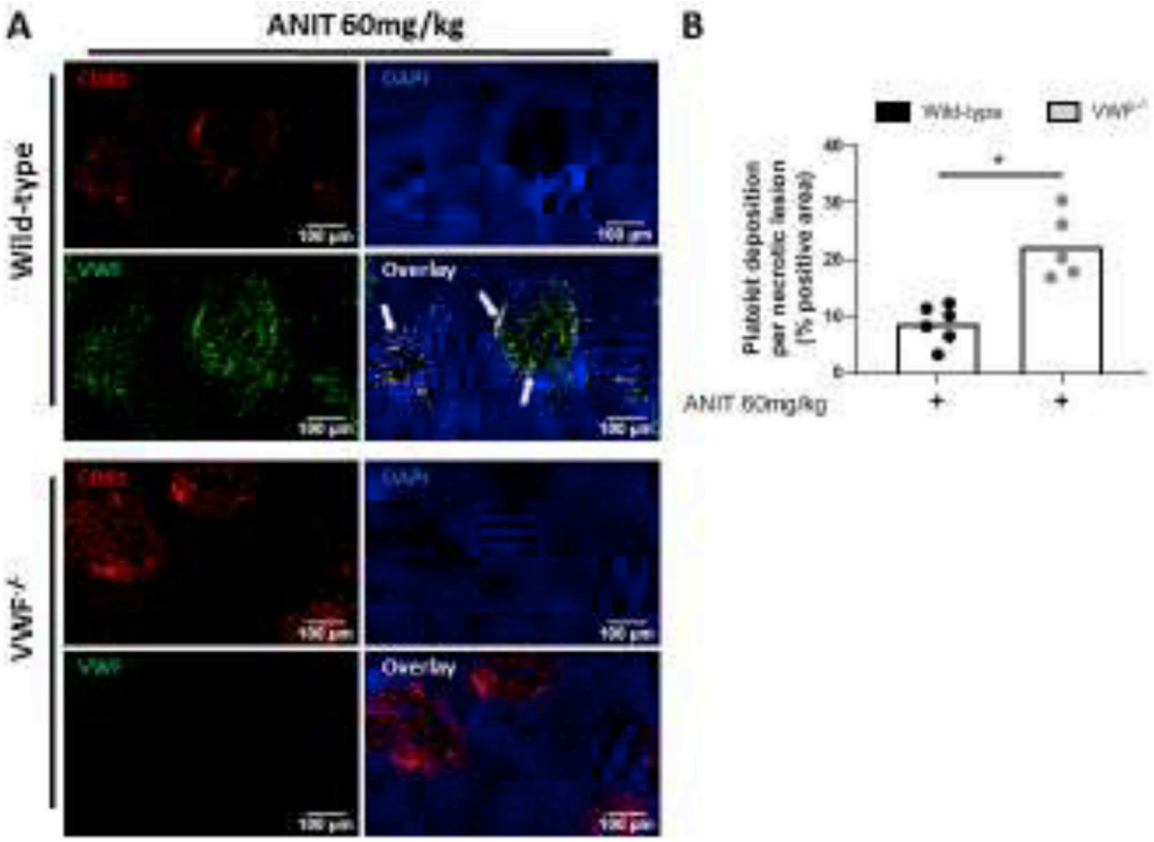

Figure 3. VWF deficiency increases hepatic platelet deposition in acute cholestatic liver injury.

Fasted female wild-type and VWF$^{-/-}$ mice were treated with ANIT (60mg/kg, p.o.) and hepatic VWF and platelet deposition assessed 48 hours later. (A) Representative images of platelets (in red), VWF (in green), and cell nuclei (in blue) in liver sections of wild-type mice (upper panels) or VWF$^{-/-}$ mice (lower panels) treated with ANIT. Co-localization of VWF with platelets is shown in yellow (marked by white arrows). (B) Quantification of hepatic platelet deposition within necrotic lesions expressed as percentage of positive pixel count per necrotic lesion. Bars represent mean and individual animals are plotted (n = 5–6 mice per group). * $p < 0.05$

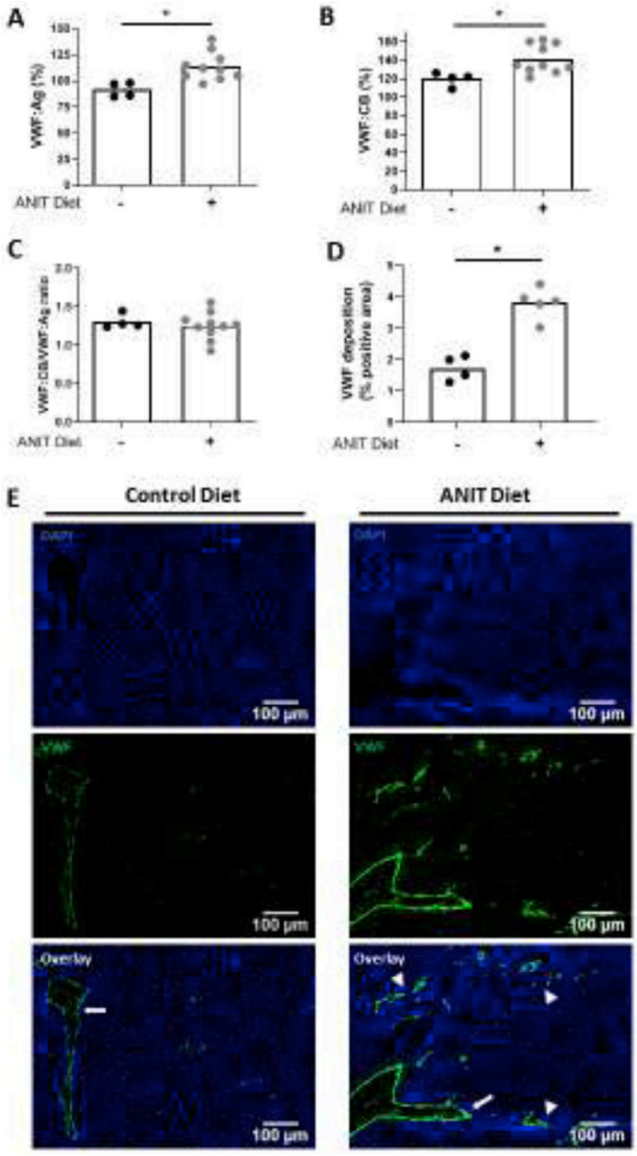

Figure 4. Impact of ANIT-induced chronic liver injury on plasma and hepatic VWF.

Female wild-type mice were fed control diet (regular chow) or diet containing 0.05% ANIT for 6 weeks. Blood was collected to assess VWF parameters in plasma and livers were collected to assess hepatic VWF deposition. (A) VWF plasma antigen (VWF:Ag) levels in wild-type mice fed control diet or ANIT diet. Levels are expressed as % of normal pooled mouse plasma which was set at 100%. (B) VWF collagen binding activity (VWF:CB) in plasma samples from wild-type-challenged mice, shown as a percentage compared with normal pooled mouse plasma, which was set at 100%. (C) Shown is the ratio between VWF:CB and VWF:Ag (VWF:CB/VWF:Ag) in plasma samples from challenged wild-type mice. (D) Quantification of hepatic VWF deposition, expressed as percentage of positive pixel count. (E) Representative images of VWF (in green) and cell nuclei (in blue) in liver sections of wild-type mice fed control diet (left panel) or ANIT containing diet (right panel). White arrows mark VWF staining of the endothelial lining, white triangles mark VWF

staining within areas of biliary hyperplasia. Bars represent mean and individual animals are plotted (n = 4–10 mice per group for panels A-C, n=4–5 mice for panel D). * $p < 0.05$

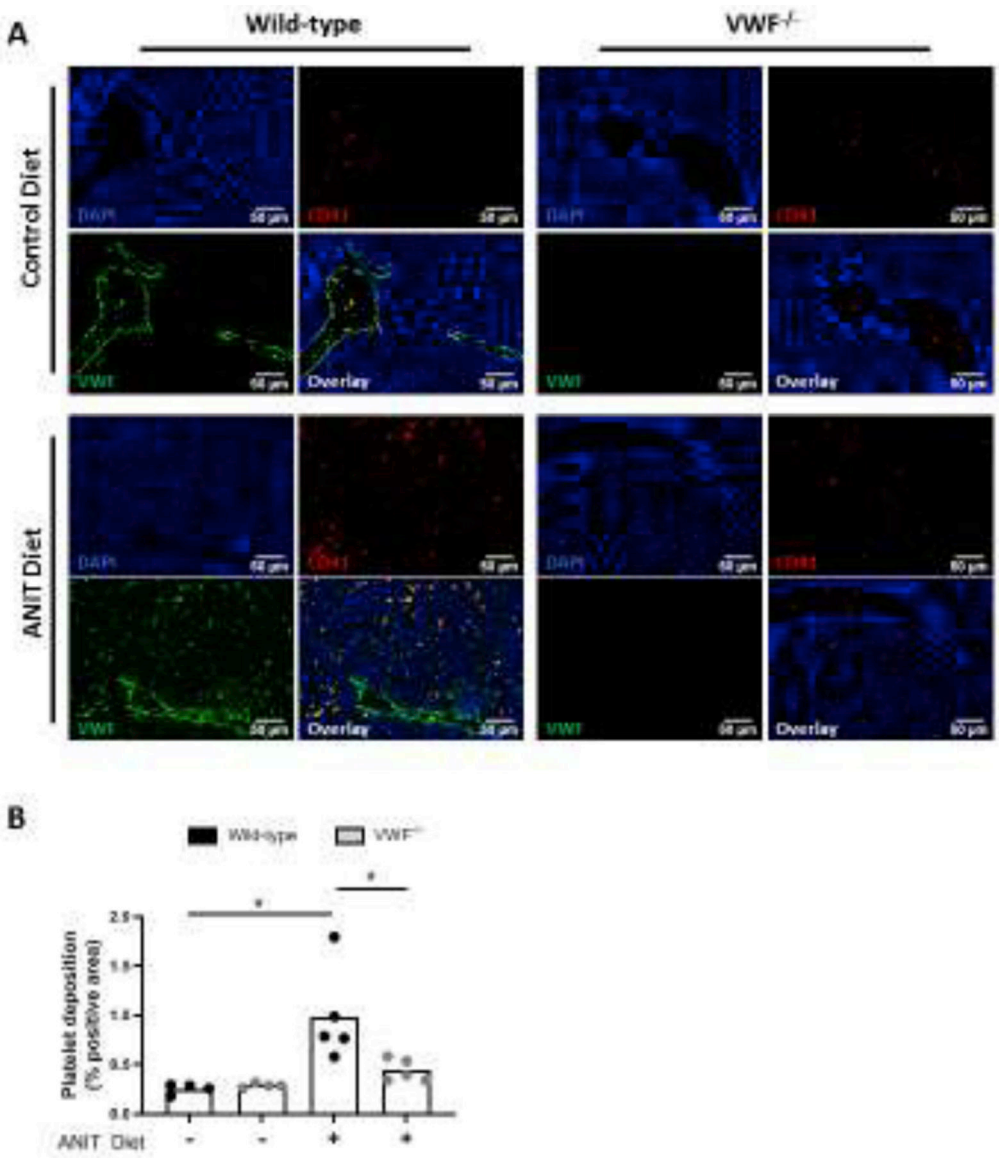

Figure 5. VWF deficiency reduces hepatic platelet accumulation after ANIT-induced chronic injury in mice.

Female wild-type and VWF$^{-/-}$ mice were fed control diet (regular chow) or diet containing 0.05% ANIT for 6 weeks. Livers were collected to assess hepatic platelet. (A) Representative images of platelets (in red) and cell nuclei (in blue) in liver sections of wild-type mice (upper panels) or VWF$^{-/-}$ mice (lower panels) fed control diet. (B) Representative images of platelets (in red) and cell nuclei (in blue) in liver sections of wild-type mice (upper panels) or VWF$^{-/-}$ mice (lower panels) fed ANIT containing diet. (C) Quantification of hepatic platelet accumulation expressed as percentage of positive pixel count. Bars represent mean and individual animals are plotted (n = 4–5 mice per group). # p <0.05 compared with control-fed mice, * p <0.05

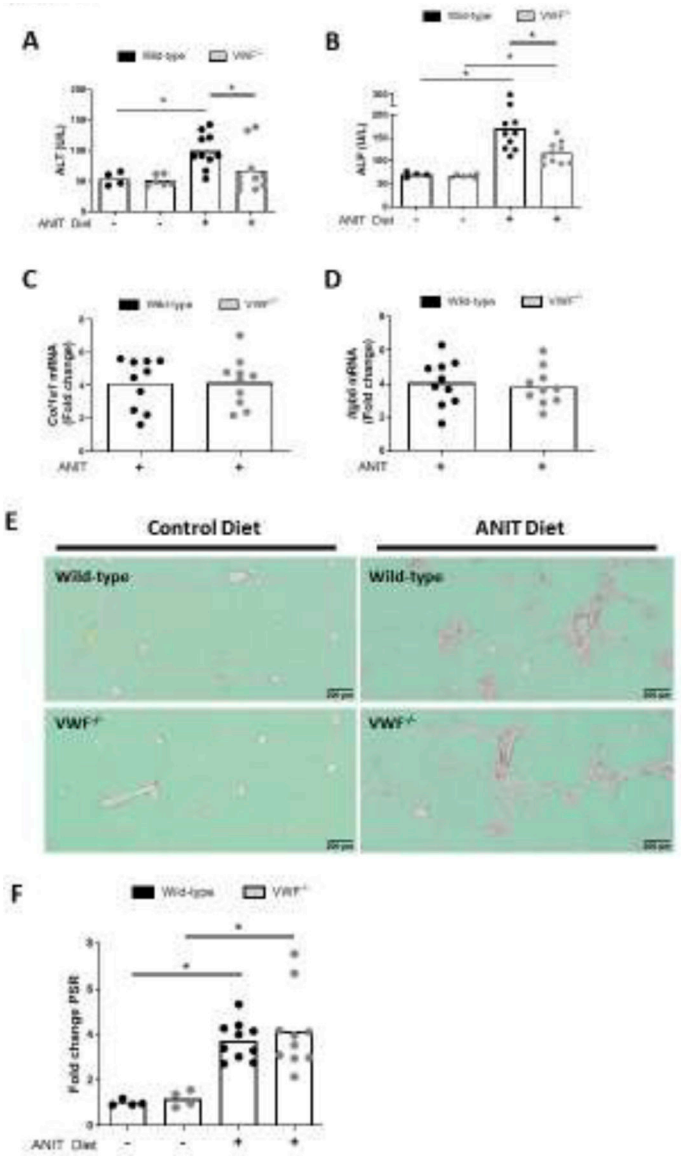

Figure 6. VWF deficiency reduces ANIT-induced liver injury but not fibrosis in mice.

Female wild-type and VWF$^{-/-}$ mice were fed control diet (regular chow) or diet containing 0.05% ANIT for 6 weeks. Blood and livers were collected to assess liver injury and biliary fibrosis. (A) Serum ALT activity in control and ANIT-fed wild-type and VWF$^{-/-}$ mice. (B) Serum ALP activity in control and ANIT-fed wild-type and VWF$^{-/-}$ mice. Hepatic mRNA expression of (C) *Col1a1* and (D) *Itgb6* in ANIT-fed wild-type and VWF$^{-/-}$ mice. (E) Representative images show liver sections stained for collagens with picrosirius red. (F) Quantification of picrosirius red staining expressed as fold change compared with control-fed wild-type mice. Bars represent mean and individual mice are plotted (n = 4–10 mice per group). * p <0.05.

Table 1.

Changes in VWF parameters and liver injury after ANIT challenge.

	Vehicles (n=7)	ANIT (n=13)	P-value
Parameter	**Mean ± SEM**	**Mean ± SEM**	
VWF:Ag (%)	84 ± 5	124 ± 13	0.046
VWF:CB (%)	83 ± 4	131 ± 14	0.022
VWF:CB/VWF:Ag ratio	1.01 ± 0.06	1.05 ± 0.03	0.408
ALT (U/L)	40 ± 4	325 ± 56	0.002
ALP (U/L)	62 ± 3	170 ± 30	0.017

VWF:Ag = von Willebrand Factor: Antigen, VWF:CB = von Willebrand factor: Collagen Binding, ALT = alanine aminotransferase, ALP = alkaline phosphatase, ANIT = α-naphthylisothiocyanate.